Measurement of the strong intracrystalline electric field in the Schwinger interaction with diffracted neutrons

V. L. Alekseev, V. V. Voronin, E. G. Lapin, E. K. Leushkin, V. L. Rumyantsev, O. I. Sumbaev, and V. V. Fedorov

B. P. Konstantinov Institute of Nuclear Physics, Leningrad, Academy of Sciences of the USSR
(Submitted 30 May 1989)
Zh. Eksp. Teor. Fiz. **96**, 1921–1926 (December 1989)

The first experimental study is reported of the Schwinger interaction between polarized neutrons and the electric field in a noncentrally symmetric crystal during dynamic two-wave diffraction. The phase shifts in the pendellösung diffraction pattern produced during the change in the orientation of the neutron spin relative to the crystallographic planes were measured for two crystals of α-quartz of different thickness. A theory of the effect is given in the two-wave approximation. The interplane electric field in which the diffracted neutrons propagate is calculated to be 2.1×10^8 V/cm for $(11\bar{2}0)$ which is in good agreement with the experimental result $(1.8\pm0.2)\times10^8$ V/cm.

INTRODUCTION

It is shown in Ref. 1 that it is possible to select relatively high-grade crystals of α-quartz in order to observe the pendellösung pattern due to thermal-neutron diffraction. As far as we know, quartz is the only perfect crystal without a center of symmetry. This offers a unique opportunity for the experimental study of the Schwinger interaction between a diffracted neutron and the relatively strong ($\sim10^8$ V/cm) interplane electric field.

The essence of the phenomenon is as follows. In a noncentrally symmetric crystal, the maxima of the nuclear potential are shifted on some planes relative to the maxima of the electric potential. The result is that neutrons described by the two Bloch waves $\psi^{(1)}$, $\psi^{(2)}$ corresponding to different branches of the dispersion surface experience strong electric fields of different sign

$$\langle\psi^{(1)}|\mathbf{E}|\psi^{(1)}\rangle=-\langle\psi^{(2)}|\mathbf{E}|\psi^{(2)}\rangle,$$

because the positions of the maxima on the neutron planes $|\psi^{(1)}|^2$ and $|\psi^{(2)}|^2$ are determined by the nuclear potential. Hence the Schwinger interaction leads to the spin dependence of the measured phase of the pendellösung pattern. The fact that the noncentrally symmetric character of the crystal had to be taken into account was previously noted in Ref. 2 and 3.

THEORY

When the Bragg condition is satisfied, the equation of the dispersion surface for a neutron in the crystal has the following form in the two-wave approximation (see, for example, Ref. 4):

$$(k^{(1,2)})^2=K\mp|U_g|, \tag{1}$$

where $k^{(1)}$, $k^{(2)}$ are the wave vectors describing the propagation of the two neutron waves $\psi^{(1,2)}$ in the crystal $K=[2m(\mathscr{E}-V_0)]^{1/2}/\hbar$, m and $\mathscr{E}$ are, respectively, the mass and the energy of the incident neutron, $U_g=2mV_g/\hbar^2$, V_g is the amplitude of the gth harmonic of the periodic crystal potential that defines the crystallographic planes $\mathbf{g}(hkl)$, $V_g=V^*_{-g}$, $\mathbf{g}$ is the reciprocal lattice vector $|\mathbf{g}|=2\pi/d$, d is the plane separation, and V_0 is the mean potential in the crystal.

The difference between the wave vectors $\mathbf{k}^{(1)}$ and $\mathbf{k}^{(2)}$ is due to the different symmetry of the neutron Bloch functions $\psi^{(1)}$ and $\psi^{(2)}$. If we write $V_g=v_g\exp(i\Phi_g)$, the functions $\psi^{(1)}$ and $\psi^{(2)}$ assume the form

$$\psi^{(1)}(\mathbf{k}^{(1)},\mathbf{r})=2^{1/2}\cos\frac{\mathbf{gr}+\Phi_g}{2}\exp\left[i\left(\mathbf{k}^{(1)}+\frac{\mathbf{g}}{2}\right)\mathbf{r}\right], \tag{2}$$

$$\psi^{(2)}(\mathbf{k}^{(2)},\mathbf{r})=2^{1/2}i\sin\frac{\mathbf{gr}+\Phi_g}{2}\exp\left[i\left(\mathbf{k}^{(2)}+\frac{\mathbf{g}}{2}\right)\mathbf{r}\right]. \tag{3}$$

The phase of Φ_g depends on the choice of the origin of coordinates.

In the symmetric Laue case (entrance face of the crystal perpendicular to the reflecting planes; see Fig. 1), the two waves $\psi^{(1)}$, $\psi^{(2)}$ excited in the crystal have equal amplitudes.

The small wave vector difference

$$\Delta k=|\mathbf{k}^{(2)}-\mathbf{k}^{(1)}|=2|V_g|/\hbar v_\parallel$$

leads to a periodic dependence of the intensities I_0, I_g of direct and diffracted beams (pendellösung) on the crystal thickness L (or neutron wavelength λ):

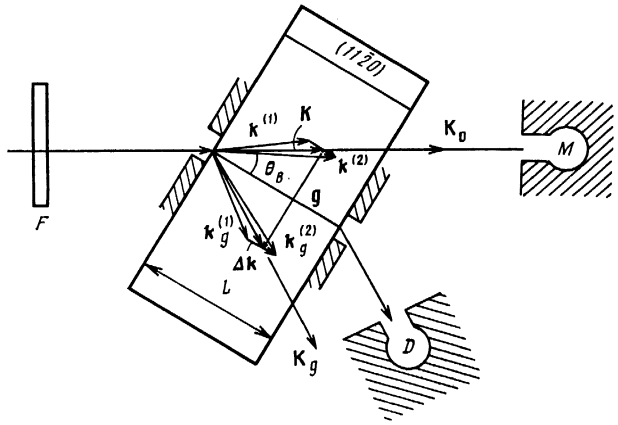

FIG. 1. Experimental set up: F—flipper, D—detector, M—beam monitor. The spin of the neutron is perpendicular to the plane of the figure; $\mathbf{k}_g^{(1,2)}=\mathbf{k}^{(1,2)}+\mathbf{g}$, $\mathbf{K}_g=\mathbf{K}+\mathbf{g}$; $\mathbf{K}=(\mathbf{k}^{(1)}+\mathbf{k}^{(2)})/2$.

 0038-5646/89/121083-03$04.00

TABLE I. Calculated values of v_g^E, $\Delta\Phi_g$, E_g for the $g(hk\bar{m}l)$ planes of α-quartz $m = h + k$.

g	$11\bar{2}1$	$11\bar{2}2$	$11\bar{2}3$	$11\bar{2}4$	$11\bar{2}5$	$10\bar{1}0$	$12\bar{3}0$	$13\bar{4}0$	$14\bar{5}0$	$15\bar{6}0$
v_g^E, V	0.96	2.24	0.99	1.42	0.87	2.42	0.60	1.54	0.079	0.30
$\Delta\Phi_g$, rad	2.12	0.036	2.88	2.98	0.27	0	0.29	0.045	0.66	1.04
E_g, 10^8 V/cm	2.31	0.28	1.10	1.11	1.48	0	0.66	0.37	0.31	2.10

$$I_{0,g} = {}^1/_2(1 \pm \cos\varphi), \tag{4}$$

where

$$\varphi = L\Delta k = 2|V_g|L/\hbar v_\parallel, \quad v_\parallel = \hbar|\mathbf{K}+\mathbf{g}/2|/m = \hbar K\cos\theta_B/m$$

is the mean neutron velocity in the crystal (along the crystallographic planes), $\mathbf{K} = (\mathbf{k}^{(1)} + \mathbf{k}^{(2)})/2$, and θ_B is the Bragg angle. For a nonmagnetic crystal, the periodic potential $V(\mathbf{r})$ of the system of crystallographic planes consists of two components, namely, the nuclear component $V^N(\mathbf{r})$ and the Schwinger component $V^S(\mathbf{r},\boldsymbol{\sigma})$. The latter is determined by the electric potential $V^E(\mathbf{r})$:

$$V^S(\mathbf{r},\boldsymbol{\sigma}) = -g_n\mu_N\frac{\boldsymbol{\sigma}[\mathbf{E}\mathbf{v}_\parallel]}{2c} = g_n\mu_N\frac{\boldsymbol{\sigma}[\nabla V^E, \mathbf{v}_\parallel]}{2c}. \tag{5}$$

where g_n is the gyromagnetic ratio of the neutron, μ_N is the nuclear magnetron $\mu_N = e\hbar/2m_pc$, m_p is the proton mass, and the magnetic moment of the neutron is $\mu = \mu_N g_n/2$.

Substituting $V_g^N = v_g^N \exp(i\Phi_g^N)$, we obtain

$$V^N(\mathbf{r}) = 2v_g^N\cos(\mathbf{gr}+\Phi_g^N). \tag{6}$$

Similarly, for $V_g^E = v_g^E\exp(i\Phi_g^E)$, we find that the electric potential becomes

$$V^E(\mathbf{r}) = 2v_g^E\cos(\mathbf{gr}+\Phi_g^E). \tag{7}$$

Substituting (7) into the Schwinger potential (5), we obtain

$$V^S(\mathbf{r},\boldsymbol{\sigma}) = -g_n\mu_N\frac{\boldsymbol{\sigma}[\mathbf{g}\mathbf{v}_\parallel]}{2c}2v_g^E\sin(\mathbf{gr}+\Phi_g^E), \tag{8}$$

from which it follows that[1)]

$$V_g^S(\boldsymbol{\sigma}) = ig_n\mu_N\frac{\boldsymbol{\sigma}[\mathbf{g}\mathbf{v}_\parallel]}{2c}v_g^E\exp(i\Phi_g^E) \equiv v_g^S\exp(i\Phi_g^S). \tag{9}$$

Finally,

$$V_g = \exp(i\Phi_g^N)\left\{v_g^N + ig_n\mu_N\frac{\boldsymbol{\sigma}[\mathbf{g}\mathbf{v}_\parallel]}{2c}v_g^E\exp(i\Delta\Phi_g)\right\}, \tag{10}$$

where $\Delta\Phi_g = \Phi_g^E - \Phi_g^N$ ($\Delta\Phi_g \equiv 0$ for a centrally symmetric crystal). We note that, in our case, $\Phi_g \approx \Phi_g^N$ because $v_g^S \ll v_g^N$.

Neglecting terms that are quadratic in the Schwinger interaction, we obtain

$$|V_g| = v_g^N + g_n\mu_N\frac{\boldsymbol{\sigma}[\mathbf{v}_\parallel\mathbf{g}]}{2c}v_g^E\sin\Delta\Phi_g. \tag{11}$$

As a result, the phase shift $\Delta\varphi$ of the pendellösung pattern due to the rotation of the neutron spin by 180° (the spin is perpendicular to the diffraction plane) is given by [see (4)]

$$\Delta\varphi = g_n e E_g L/m_p c^2, \tag{12}$$

where

$$E_g = v_g^E(2\pi/d)\sin\Delta\Phi_g = |\langle\psi^{(1,2)}|\mathbf{E}|\psi^{(1,2)}\rangle|$$

is the mean electric field acting on the diffracted neutron in the crystal.

Substituting $v^E_{11\bar{2}0} = 1.89$ V, $\Delta\Phi_{11\bar{2}0} = 0.46$, $d = 2.46\cdot10^{-8}$ cm, and using tabulated values of the parameters of the α-quartz, we find that, to within 10%,

$$E_{11\bar{2}0} = 2.14\cdot10^8 \text{ V/cm}.$$

Table I lists the corresponding calculated values for a number of other planes. The 10% uncertainty is nearly the maximum figure and is largely due to the uncertainty in the ionicity of the silicon-oxygen bond ($i \approx 0.5$) which affects the Coulomb form factors.

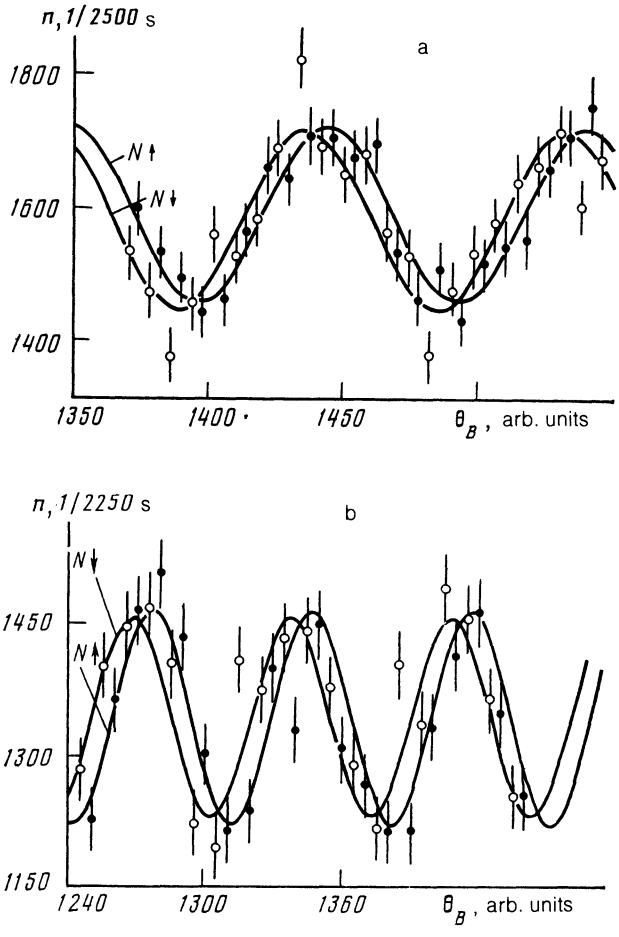

FIG. 2. Experimental pendellösung pattern for oppositely polarized neutrons ($N\uparrow$, $N\downarrow$). The quartz crystal ($11\bar{2}0$) had thickness (a) $L_\text{I} = 0.80$ cm; (b) $L_\text{II} = 1.14$ cm. Approximately one quarter of all the accumulated data are shown.

TABLE II. Measured phase shifts in the pendellösung pattern.

$\Delta\varphi_P$	$\Delta\varphi_{\text{norm}}$	Note
	$L_{\text{I}}=0.80$ cm	
(+27.0±7.1)°	(+36.0±9.5)°	$P=0.75\pm0.05$
(−25.1±5.2)°	(−33.5±6.9)°	$P=0.75\pm0.05$
		Crystal rotated by 180° relative to the normal to large face
(+26.8±9.5)°	(+34±12)°	
		Crystal returned to original position
(+0.7±6.5)°	–	Control experiment with a shim
	$L_{\text{II}}=1.14$ cm	
(+28.2±6.2)°	(+35.3±7.8)°	$P=0.80\pm0.05$
(−45.6±6.1)°	(−57.0±7.6)°	$P=0.80\pm0.05$
		Crystal rotated by 180° relative to the normal to large face

EXPERIMENT

The experimental set up is shown in Fig. 1. The polarized neutron beam ($P = 0.75$–0.80 for $\lambda = 1.8$–2.2 Å) is incident at the Bragg angle on a crystal of natural quartz with the $(11\bar{2}0)$ reflecting planes perpendicular to the entrance and exit faces. Two slabs of thickness $L_{\text{I}} = 0.8$ cm and $L_{\text{II}} = 1.14$ cm were cut. The beam spot on the entrance face was 0.06×1.66 cm^2. The exit slit (0.06 cm) was placed accurately at the center of the Borrman cell. This means that the detector recorded neutrons for which the Bragg condition was accurately satisfied. The quality of the crystals was tested by the γ-ray diffraction method.[6] The effective mosaic size was found to be $\omega_{\text{eff}} = 0.1''$–$0.2''$.

Figure 2 shows typical experimental pendellösung patterns (diffracted-beam intensity as a function of the Bragg angle θ_B). They were obtained by varying the Bragg angle by $\theta_B - 2\theta_B$ scanning. The Bragg angle θ_B is plotted along the horizontal axis (one relative unit corresponds to 10″) and the vertical axis shows the total intensity n (including the background) obtained in an exposure of 2500 s per point. The two pendellösung patterns correspond to the two opposite polarizations $N\uparrow$ and $N\downarrow$. The coil flipper F reverses the sign of the polarization after each point on the curve. The measured values are listed in Table II in which the first column gives the phase shifts $\Delta\varphi_P = \varphi_P(N\uparrow) - \varphi_P(N\downarrow)$ for different positions of the crystal (defined in the third column). A rotation of the crystal around the normal by 180° should alter the sign of $\Delta\varphi$ and this is confirmed by our experiment (rows 2 and 6 in Table II). The second column of Table II lists the values of $\Delta\varphi_{\text{norm}}$ normalized to $P = 1$.

The values of the average $|\Delta\varphi^{\text{exp}}_{11\bar{2}0}|$ and of the corresponding root mean square uncertainties obtained for the two crystals are as follows:

$$|\Delta\varphi^{\text{exp}}_{11\bar{2}0}|_{L_{\text{I}}} = (34.3\pm5.1)^\circ, \quad |\Delta\varphi^{\text{exp}}_{11\bar{2}0}|_{L_{\text{II}}} = (46\pm11)^\circ.$$

Using these results, the thicknesses L_{I}, L_{II}, and the universal constants, we obtain from (12) the following experimental values for the interplane electric field:

$$E^{\text{exp(I)}}_{11\bar{2}0} = (1.8\pm0.3)\cdot10^8\ \text{V/cm},$$

$$E^{\text{exp(II)}}_{11\bar{2}0} = (1.7\pm0.4)\cdot10^8\ \text{V/cm}.$$

The final result is as follows: $E^{\text{exp}}_{11\bar{2}0} = (1.8\pm0.2)\cdot10^8$ V/cm. This experimental value is in good agreement with the above theoretical interplane field. This field is stronger by a factor 10^3–10^4 than the electric field that can be produced in the laboratory.

[1)] The expression given by (9) can also be derived as the structure amplitude for scattering by the spin-orbit potential of an atom.[3,5] Note also that we have neglected the Foldy, weak, and other small corrections to the interaction.

[1] V. L. Alekseev, E. G. Lapin, E. K. Leushkin *et al.*, Zh. Eksp. Teor. Fiz. **94**, (8) 371 (1988) [Sov. Phys. JETP **67**, 1727 (1988)].
[2] Yu. G. Abov, A. D. Gul'ko, and P. A. Krupchitskiĭ, *Polarized Slow Neutrons* [in Russian], Atomizdat, Moscow, 1966, p. 256.
[3] M. Forte, J. Phys. G **9**, 745 (1983).
[4] P. B. Hirsch, A. Howie, R. B. Nicholson, D. W. Pashley, and M. Whelan, *Electron Microscopy of Thin Crystals*, Butterworth, London, 1965 [Russ. transl., Mir, Moscow, 1968].
[5] C. Stassis and J. A. Oberteuffer, Phys. Rev. **10**, 5192 (1974).
[6] V. L. Alekseyev, A. I. Kurbakov, and V. I. Trunov, Preprint No. 1345, Leningrad Institute of Nuclear Physics, 1987.

Note added in proof (1 November 1989). A similar[3] but more detailed theory of effects associated with spin rotation and dichroism during neutron diffraction in noncentrally symmetric crystals has been given by V. G. Baryshevskiĭ and S. V. Cherepitsa [Phys. Stat. Sol. (b) **128**, 379 (1985)].

Translated by S. Chomet